Human Molecular Genetics, 2016, Vol. 25, No. 13 2738–2751

doi: 10.1093/hmg/ddw131
Advance Access Publication Date: 30 April 2016
Original Article

ORIGINAL ARTICLE

Deletion of CTNNB1 in inhibitory circuitry contributes to autism-associated behavioral defects

Fengping Dong[1,†], Joanna Jiang[1,†], Colleen McSweeney[1], Donghua Zou[1,2], Long Liu[1,3] and Yingwei Mao[1,*]

[1]Department of Biology, Pennsylvania State University, University Park, PA 16802, USA, [2]Department of Neurology, First Affiliated Hospital, Guangxi Medical University, Nanning, Guangxi Province, 530021, China and [3]Department of Chemistry and Biology, College of Science, National University of Defense Technology, Changsha, Hunan Province 410073, China

*To whom correspondence should be addressed at Department of Biology, Pennsylvania State University, University Park, PA 16802, USA. Tel: +814-321-4739; Fax: +814-863-1357. Email: yzm1@psu.edu

Abstract

Mutations in β-catenin (CTNNB1) have been implicated in cancer and mental disorders. Recently, loss-of-function mutations of CTNNB1 were linked to intellectual disability (ID), and rare mutations were identified in patients with autism spectrum disorder (ASD). As a key regulator of the canonical Wnt pathway, CTNNB1 plays an essential role in neurodevelopment. However, the function of CTNNB1 in specific neuronal subtypes is unclear. To understand how CTNNB1 deficiency contributes to ASD, we generated CTNNB1 conditional knockout (cKO) mice in parvalbumin interneurons. The cKO mice had increased anxiety, but had no overall change in motor function. Interestingly, CTNNB1 cKO in PV-interneurons significantly impaired object recognition and social interactions and elevated repetitive behaviors, which mimic the core symptoms of patients with ASD. Surprisingly, deleting CTNNB1 in parvalbumin-interneurons enhanced spatial memory. To determine the effect of CTNNB1 KO in overall neuronal activity, we found that c-Fos was significantly reduced in the cortex, but not in the dentate gyrus and the amygdala. Our findings revealed a cell type-specific role of CTNNB1 gene in regulation of cognitive and autistic-like behaviors. Thus, this study has important implications for development of therapies for ASDs carrying the CTNNB1 mutation or other ASDs that are associated with mutations in the Wnt pathway. In addition, our study contributes to a broader understanding of the regulation of the inhibitory circuitry.

Introduction

Autism spectrum disorder (ASD) is a class of neurodevelopmental disorders characterized by persistent deficits in social communication and social interaction (1). Patients with ASD often have an increased risk of anxiety (2) and memory deficits (3). The prevalence of ASD is on the rise, and no effective treatments exist. Although the etiology is not completely known, many genetic factors are associated with ASDs (4). Both structural chromosomal changes (chromosomal translocation and copy number variations) and single-gene mutations lead to ASD-related clinical manifestations (5). Recent exome sequencing revealed that many *de novo* nonsense mutations

[†]These authors contributed equally to this work.
Received: January 16, 2016. **Revised:** March 22, 2016. **Accepted:** April 25, 2016

significantly increase the risk for ASD. Intriguingly, *de novo* mutations are enriched in genes that participate in the Wnt pathway, suggesting that the Wnt signaling pathway represents a convergence of the genetic risks in ASD (6). CTNNB1 is a fundamental component of the canonical Wnt signaling pathway and controls cell growth and cell adhesion (7,8). Consistently, nonsense and missense mutations in CTNNB1 were identified in patients with ASD (6) and intellectual disability (ID) (9). CTNNB1 directly interacts with multiple top ASD risk genes within the ASD genetic network (6). That analysis implicated CTNNB1 as an important modulator among 22 ASD risk genes.

Dysregulation of CTNNB1 leads to abnormal brain development (10–12) and defective dendritic morphogenesis (13,14). By interacting with N-cadherin, CTNNB1 shapes synaptic structure (15,16) and regulates excitatory postsynaptic strength (17,18). In addition, the axonal localization and translation of CTNNB1 modulate presynaptic vesicle release (19–21). As a consequence, abnormal levels of CTNNB1 in different brain regions or circuits lead to impaired memory (22–24), and a depression-like phenotype (25). Consistent with the hypothesis that the Wnt signaling is a convergent pathway for ASD, several mouse models with deletions in genes involved in the Wnt pathway show deficiencies in social interaction and repeteative behaviors (26–28). However, the circuitry mechanisms for how CTNNB1 dysfunction leads to the pathogenesis of ASD are largely unknown.

An imbalance of excitatory and inhibitory signals has been implicated in the pathophysiology of ASD. As a major type of GABAergic interneurons, parvalbumin-positive (PV+) interneurons generate fast-spiking inhibitory output (29). Cell densities of GABAergic interneurons, including PV-, calbindin-, and calretinin-positive neurons, are changed in postmortem brains of autism patients (30,31). GAD67 and GAD65, the enzymes required for GABA synthesis, are altered in autism (32,33), and PV neuron abnormality was found in different mouse models of autism (34,35). Particularly, PV knockout mice have behavioral phenotypes similar to all three core symptoms in human ASD patients (36), suggesting PV interneurons represent a major neuron type that mediates ASD pathophysiology. Interneuron deficits have been reported in several psychiatric disorders, including schizophrenia and ASDs (37).

The Wnt signaling pathway is required for proper interneuron development. However, the behavioral function of CTNNB1 in PV interneurons has not been identified. Here we established a CTNNB1 conditional knockout (cKO) mouse specifically in PV interneurons and showed that CTNNB1 cKO mice have increased anxiety, impaired cognition and social interactions, and elevated repetitive behaviors, which mimic some core symptoms of patients with ASD. Interestingly, CTNNB1 deletion in PV-interneurons enhances spatial memory and alters the neuronal activity in the cortex.

Results

CTNNB1 knockout changes the distribution of PV$^+$ interneurons

To gain new insight into CTNNB1's functions in inhibitory neural circuits, we selectively eliminated CTNNB1 by Cre-dependent deletion of *lox*P flanked exons 2 and 6, which leads to an unstable protein (12). CTNNB1$^{flox/flox}$ mice were mated with PV-Cre mice to generate mice with CTNNB1 cKO in PV interneurons. CTNNB1$^{flox/flox}$ mice were used as controls because they express normal levels of CTNNB1 (12). Mice with genotypes of CTNNB1$^{flox/flox}$ and PV-Cre; CTNNB1$^{flox/flox}$ were selected for behavior tests. All mice tested were born within 5 days, and behavioral tests started after postnatal day 60 (P60). Immunofluorescent staining confirmed that CTNNB1 was deleted from most PV+ neurons (Fig. 1A). A few PV+ neurons still expressed CTNNB1 probably due to incomplete recombination by cre recombinase. As PV is expressed postnatally (38), we further tested how deletion of CTNNB1 affects the distribution of PV interneurons. Intriguingly, the density of PV+ neurons in the prefrontal cortex was significantly higher in CTNNB1 cKO mice (Fig. 1B). However, the percentages of PV+ neurons in different hippocampal regions, the amygdala, and the hypothalamus were not changed (Fig. 1C and D), suggesting the alteration is region-specific. To gain more insights on the developmental distribution of PV+ neurons, we found that at an early developmental time, postnatal day (P22), the localization of PV+ interneurons was not changed by CTNNB1 cKO in the cortex (Supplementary Material, Fig. S1A and B) or the hippocampus (Supplementary Material, Fig. S1C), suggesting that mislocalization of PV cells occurs between P22 and P60.

CTNNB1 cKO in PV interneurons increases anxiety but not depression-related behavior

To determine if CTNNB1 cKO in PV interneurons affects any motor function, we examined them in the open field test (OFT). PV-Cre; CTNNB1$^{flox/flox}$ mice and controls had no differences in total distance travelled (Fig. 2A), speed (Supplementary Material, Fig. S2A and B), total time mobile (Supplementary Material, Fig. S2C), and total vertical rearing activity (Supplementary Material, Fig. S2D). In addition, the rotarod test showed no significant difference between the groups (Supplementary Material, Fig. S3). These data demonstrated that PV-Cre; CTNNB1$^{flox/flox}$ mice had no deficits in motor coordination and locomotor function. However, significant differences were detected on center duration time, center distance traveled, frequency and latency of center entry. In the OFT, PV-Cre; CTNNB1$^{flox/flox}$ mice had significantly less center distance traveled ($P = 0.01$) (Fig. 2B), with similar velocities ($P = 0.76$) (Fig. 2C). In the 5-min test, PV-Cre; CTNNB1$^{flox/flox}$ mice spent less time in the center region ($P = 0.03$) (Fig. 2D). PV-Cre; CTNNB1$^{flox/flox}$ mice showed less center entry ($P = 0.02$) (Fig. 2E) and a longer latency to enter the center region ($P = 0.005$) (Fig. 2F). The evidence from of OFT showed that mice with CTNNB1 cKO in PV neurons avoid traveling in the center region (Fig. 2G), suggesting an increase of anxiety in CTNNB1 cKO mice.

To confirm the elevated anxiety-like behaviors in CTNNB1 cKO mice, we used the elevated plus maze (EPM), a well-established test for assessing anxiety responses in rodents (39). PV-Cre; CTNNB1$^{flox/flox}$ mice showed a significant difference on the latency of arms entry compared to littermate controls. It took much longer ($P = 0.048$) for CTNNB1 cKO mice to enter open arms (Fig. 3A). They entered the closed arms much earlier ($P = 0.002$) than the CTNNB1$^{flox/flox}$ mice (Fig. 3A), suggesting that cKO mice are more anxious. CTNNB1$^{flox/flox}$ mice showed a similar frequency entering either open or closed arms (Fig. 3B). However, PV-Cre; CTNNB1$^{flox/flox}$ mice preferred the closed arms more often than the open arms ($P = 0.0007$), and they entered the closed arms more frequently than the control mice ($P = 0.014$) (Fig. 3B). Although two groups traveled similar total distance in closed and open arms (Fig. 3C), the distance traveled in the open arm was much less than in the PV-Cre; CTNNB1$^{flox/flox}$ mice ($P = 0.06$) (Fig. 3C and E). CTNNB1 cKO mice spent similar time in open and closed arms as littermate controls

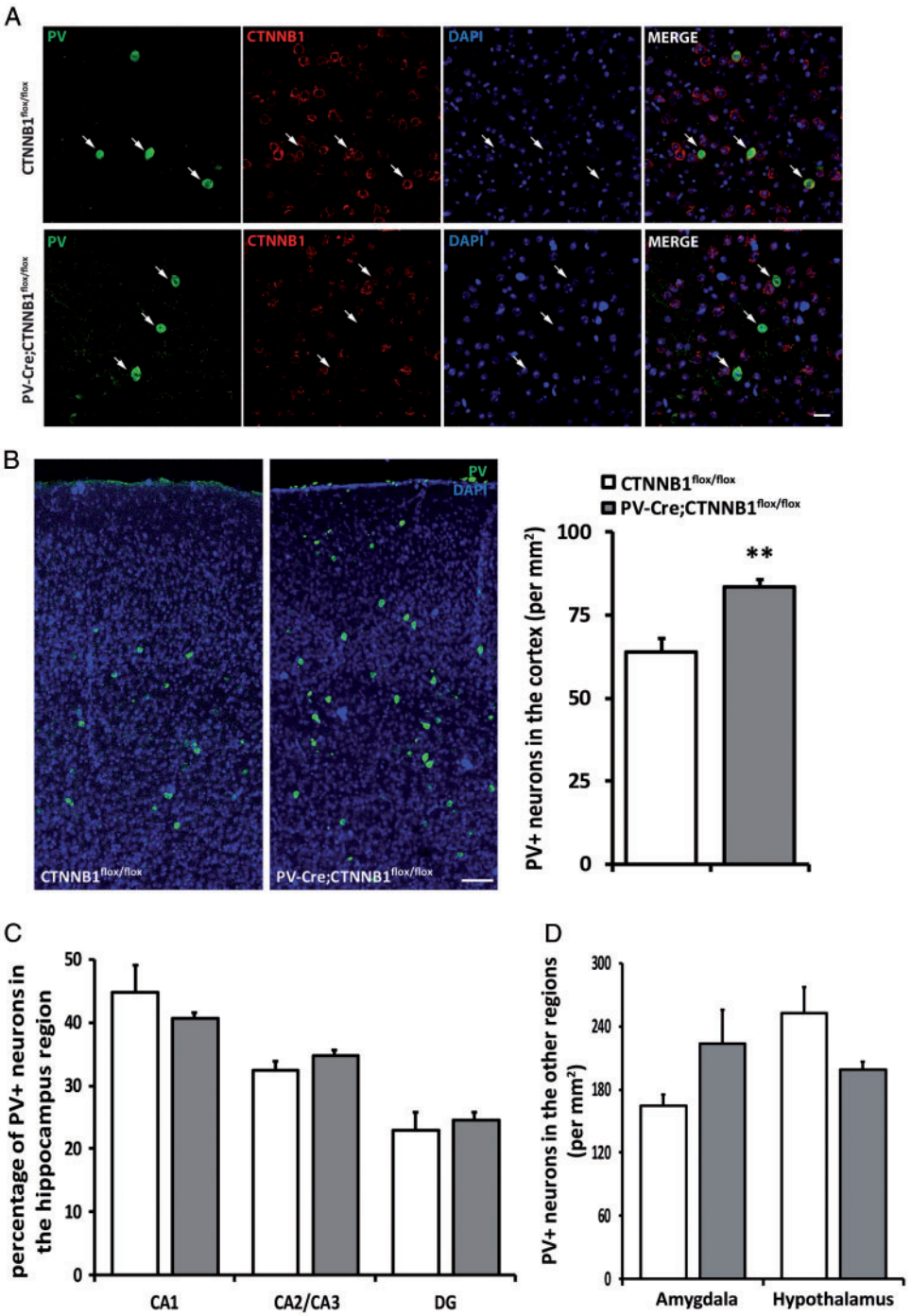

Figure 1. Abnormal arrangement of PV-positive cells in PV-Cre; CTNNB1$^{flox/flox}$ mice. **(A)** Immunofluorescent staining of CTNNB1 in PV+ cells. White arrows indicate PV-positive cells (green). CTNNB1 expression was present in control mice, but was absent in PV-Cre; CTNNB1$^{flox/flox}$ mice. Scale bar = 10 μm. **(B)** PV-Cre; CTNNB1$^{flox/flox}$ mice (N = 4) showed significant more PV$^+$ cells (green) in the prefrontal cortex than CTNNB1$^{flox/flox}$ mice (N = 6). Scale bar = 100 μm. **(C)** Similar percentages of PV+ neurons were detected in the hippocampal regions. **(D)** Similar number of PV+ neurons were localized at the amygdala and the hypothalamus . *$P < 0.05$, **$P < 0.01$.

(Supplementary Material, Fig. S4A). Although it did not reach significance, they tended to spend more time in the center region ($P = 0.08$) and less time in the distal half of the open arms ($P = 0.07$) (Supplementary Material, Fig. S4B). Consistent with increased anxiety-like behaviors, CTNNB1 cKO mice were reluctant to enter the distal half of the open arms ($P = 0.02$) (Supplementary Material, Fig. S4C). Head-dipping is a compulsive-like behavior that is a high risk for anxiety (39,40). PV-Cre; CTNNB1$^{flox/flox}$ mice significantly increased their head-dipping behavior ($P = 0.047$), especially at the center region of the plus maze apparatus ($P < 0.001$) (Fig. 3D). Rearing behavior did not significantly increase in our test (Supplementary Material, Fig. S4D). It may be that PV-Cre; CTNNB1$^{flox/flox}$ mice traveled less in the open arms. Our results from the OFT and EPM indicated that CTNNB1 KO in PV$^+$ neurons leads to an increase of anxiety behaviors.

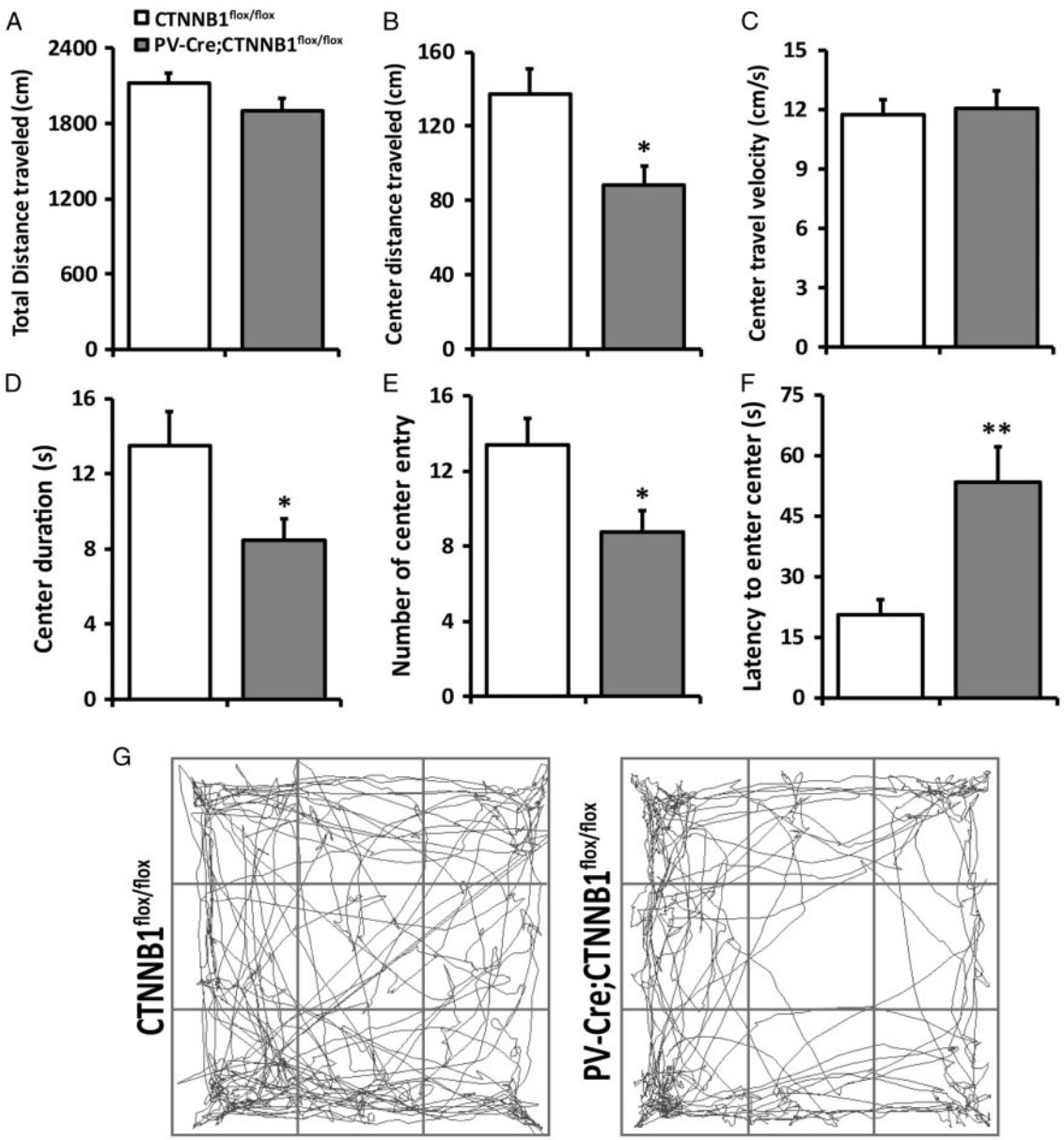

Figure 2. PV-Cre; CTNNB1$^{flox/flox}$ mice display anxiety-like behavior. **(A)** In the OFT, two groups of mice traveled similar total distances. **(B)** PV-Cre; CTNNB1$^{flox/flox}$ mice travelled less in the center. **(C)** Velocity in the center. **(D)** PV-Cre; CTNNB1$^{flox/flox}$ mice spent less time in the center than controls. **(E)** Center entry. **(F)** Latency for the first entry into the center. **(G)** Schematics showed the zone setting and representative traces of mouse movement. Data shown are mean ± SEM from CTNNB1$^{flox/flox}$ (N = 18) and PV-Cre; CTNNB1$^{flox/flox}$ groups (N = 10). *$P < 0.05$, **$P < 0.01$.

The tail suspension test assesses the efficacy of antidepressant drugs and determines depression-related behavior in genetic mouse models (41). In this test, the depression-related behavior of our mice was not affected (Supplementary Material, Fig. S5). The immobile time (lack of struggle-related behavior) was not significantly altered in CTNNB1 cKO mice ($P = 0.237$).

CTNNB1 cKO in PV neurons alters recognition performance

Because mutations in CTNNB1 result in IDs (9) and PV interneurons modulate cognitive functions (42), we tested how CTNNB1 defects in PV interneurons alter cognitive function and memory. Using the novel object recognition (NOR) test, mice were exposed to different objects after acclimation to a pair of identical objects. No significant difference was found between CTNNB1 cKO mice and control littermates when interacting with two identical objects (Supplementary Material, Fig. S6A and B), suggesting that the presence of objects did not alter their exploratory behaviors. One hour after acclimation, one familiar object was replaced with a novel object. Both groups of mice showed increased interest in the novel object. Both interactive duration and frequency of novel object were higher than with the familiar object (Fig. 4A and B). These data suggest that CTNNB1 cKO mice maintain normal short-term memory (1 h). After 24 h, the animals were retested when novel object 1 was paired with novel object 2. The control mice spent significantly more time with the novel object 2 ($P = 0.028$) (Fig. 4C), suggesting that they

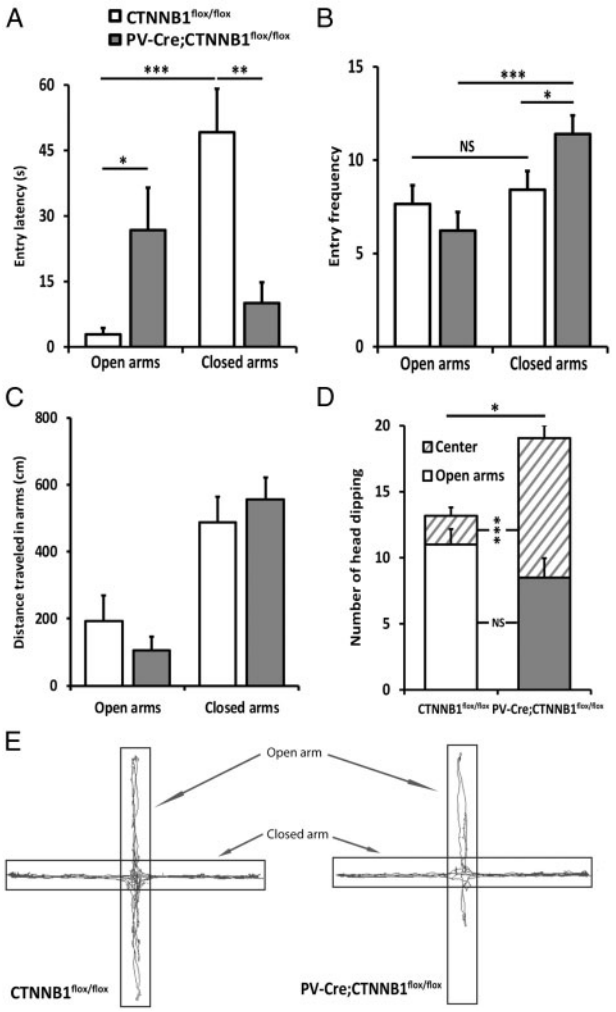

Figure 3. PV-Cre; CTNNB1$^{flox/flox}$ mice increase anxiety-like behavior. **(A)** In the EPM test, PV-Cre; CTNNB1$^{flox/flox}$ mice showed longer latency to enter open arms and shorter latency to enter closed arms. **(B)** PV-Cre; CTNNB1$^{flox/flox}$ mice were prone to enter closed arms more frequently. **(C)** PV-Cre; CTNNB1$^{flox/flox}$ mice showed a trend to travel less in open arms. **(D)** PV-Cre; CTNNB1$^{flox/flox}$ mice showed significantly more head-dipping behavior. **(E)** Schematics show the zones of the EPM and representative traces of mouse movement. Data shown are mean ± SEM from the CTNNB1$^{flox/flox}$ (N = 18) and PV-Cre; CTNNB1$^{flox/flox}$ groups (N = 10). *P < 0.05, **P < 0.01, ***P < 0.001, NS, non-significant.

retained long-term memory. However, PV-Cre; CTNNB1$^{flox/flox}$ mice had similar interactive durations and frequencies between novel object 2 and the familiar object ($P = 0.9$) (Fig. 4C, Supplementary Material, Fig. S6C). The NOR test indicated that CTNNB1 cKO from PV$^+$ neurons affected the long-term recognition but not the short-term memory.

PV interneurons synchronize spiking activity in neuronal networks and modulate fear memory (43,44). Because long-term recognition memory was changed in CTNNB1 cKO mice, we examined fear memory with a fear conditioning and extinction paradigm. No significant difference was detected in the contextual fear conditioning test during the first 2 days, suggesting that the CTNNB1 cKO mice had an intact fear memory. Interestingly, CTNNB1 cKO mice retained a high freezing percentage, and control littermates showed significant reduced extinction formation on day 3 (Fig. 4D). These data indicate that CTNNB1 cKO in PV+ neurons did not change the contextual fear condition. However, memory extinction was impaired as new memories cannot be formed in CTNNB1 cKO mice.

PV-Cre; CTNNB1$^{flox/flox}$ mice exhibits enhanced spatial memory

Several autistic mouse models showed abnormal spatial memory (45–49). We used the Morris water maze (MWM) assay to measure spatial memory. Within 4 training days, PV-Cre; CTNNB1$^{flox/flox}$ mice took less time (Fig. 5A) and swam shorter distances (Fig. 5B) to reach the platform. They also showed a higher percentage of successful rate of finding the hidden-platform within 60 s (Fig. 5C). On the testing day, after the platform was removed, we measured the time spent in the four quadrants, based on the position of the platform. PV-Cre; CTNNB1$^{flox/flox}$ mice showed decreased travel distance ($P = 0.003$) (Fig. 5D), longer duration ($P = 0.03$) (Fig. 5F) and greater travel frequency ($P = 0.02$) (Fig. 5G) into the platform quadrant than control littermates. Furthermore, to better quantify spatial memory, we used a three-zone assessment with concentric circles of different diameters surrounding the platform (Fig. 5E). Interestingly, PV-Cre; CTNNB1$^{flox/flox}$ mice showed better navigation to the target. They had significantly shorter latencies to reach the smallest target zone ($P = 0.02$), spent significantly longer time ($P = 0.02$), and entered more ($P = 0.01$) in the target zones (Fig. 5H–J). These indicate that PV-Cre; CTNNB1$^{flox/flox}$ mice can memorize the position of the platform in relation to spatial cues with higher accuracy.

CTNNB1 cKO in PV neurons alters social behaviors and increased repetitive behaviors

ASD is characterized by social-interaction difficulties and repetitive behaviors. The social interaction test (SIT) uses a three-chamber paradigm to examine social memory and social novelty in mice. Both groups of mice showed no preference for empty chambers during the habituation (Supplementary Material, Fig. S7A). When a mouse is presented with an empty chamber, both control ($P < 0.001$) and PV-Cre; CTNNB1$^{flox/flox}$ mice ($P < 0.01$) preferred to interact more with the mouse rather than the empty chamber (Fig. 6A and B), suggesting that both groups of mice maintain normal social motivation. In the second session, an unfamiliar mouse, was introduced in the empty chamber. The CTNNB1$^{flox/flox}$ mice preferred to interact with the unfamiliar mouse with significant higher interacting time ($P < 0.001$) and frequency ($P = 0.015$) (Fig. 6C–E). In contrast, PV-Cre; CTNNB1$^{flox/flox}$ mice failed to show social novelty behavior in this session.

Another core symptom of ASD is repetitive behavior. To determine if CTNNB1 cKO in PV+ neurons leads to changes of repetitive behavior, we measured the total grooming time in a testing session of 25 min. CTNNB1 cKO mice had significantly more grooming time than their control littermates ($P = 0.033$) (Fig. 7A). The marble burying test (MBT) has been used to study stereotypic behaviors related to obsessive-compulsive disorder (50), which also reflects a repetitive and perseverative behavior in ASD patients. PV-Cre; CTNNB1$^{flox/flox}$ mice took more time to start to bury the marbles ($P = 0.046$) (Fig. 7B). This result may also reflect increased anxiety in CTNNB1 cKO mice. Yet the final number of buried marbles was not statistically different in the two groups ($P = 0.758$) (Supplementary Material, Fig. S8). Thus, CTNNB1 cKO mice dug more frequently in a shorter active period. Some autism mouse models also showed problems with

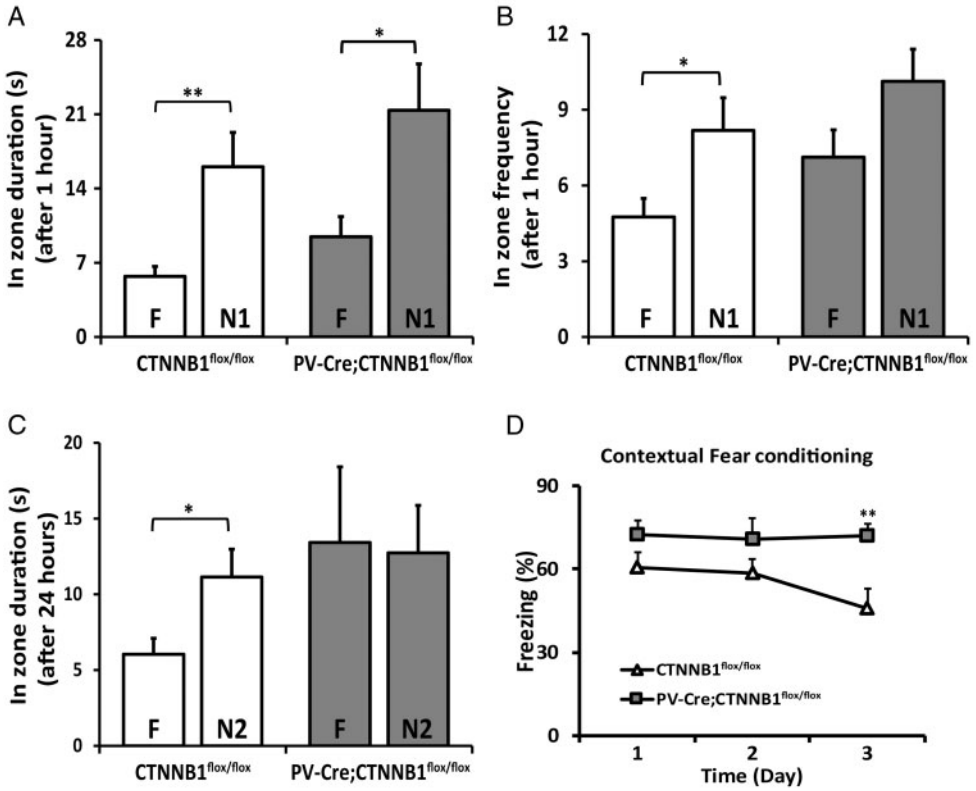

Figure 4. PV-Cre; CTNNB1$^{flox/flox}$ mice show memory deficits in the NOR test. **(A)** Both groups of mice interacted with a novel object longer than a familiar object after 1 h. **(B)** Both groups of mice were prone to interact with novel object more frequently than a familiar object after 1 h. **(C)** After replacing to another novel object in 24 h, CTNNB1$^{flox/flox}$ mice spent more time on novel object 2, but PV-Cre; CTNNB1$^{flox/flox}$ showed no preference. **(D)** In the contextual fear conditioning freezing test, PV-Cre; CTNNB1$^{flox/flox}$ mice did not decrease the percentage of freezing at the third day of extinction tests. Data shown are mean ± SEM from the CTNNB1$^{flox/flox}$ (N = 18) and PV-Cre; CTNNB1$^{flox/flox}$ groups (N = 10). *$P < 0.05$, **$P < 0.01$. F, familiar object. N1, novel object 1, N2, novel object 2.

nest building (51). Nesting has been reported to be related with defects in the septum or the hippocampus (52,53). PV-Cre; CTNNB1$^{flox/flox}$ mice performed worse on nest building test than control mice at different times. The scores were significant lower at 1 ($P = 0.02$) or 24 ($P = 0.04$) h after setting up the nesting (Fig. 7C). Moreover, we have tested the effect of gender in several behavioral tests (Supplementary Material, Figs. S2E–H, S4E–G and S7B). There is no significant difference between females and males with the same genotype. Between different genotypes, both males and female went the same direction in several tests. Thus, we believe that it will not affect our interpretation when grouping them together. Our data suggest that CTNNB1 KO in PV+ neurons alter the neuronal network and lead to autistic-like behaviors.

CTNNB1 cKO in PV neurons modulates neuronal activity in the cortex

Three forebrain structures, the prefrontal cortex, the amygdala and the hippocampus, form a dynamic neuronal network to regulate anxiety-related behaviors and modulate social interaction (54). To determine the effect of CTNNB1 KO in overall neuronal activity, we sought to determine c-Fos expression in the three brain regions of awake animals. Under a stimulated condition, in which the mice received a brief foot shot 1 h before sacrifice, we found that c-Fos positive cells was significantly reduced in the prefrontal cortex (Fig. 8A), but not in the hippocampus subregions and the amygdala of CTNNB1 cKO mice (Fig. 8B and C). Particularly, majority of c-Fos+ cells were detected in the layer II ($P = 0.03$) and V ($P = 0.006$) of the prefrontal cortex. In either layer c-Fos+ cells were significantly decreased in cKO mice (Fig. 8A), suggesting an elevated level of inhibition. Although a similar damping trend was observed in the amygdala ($P = 0.07$) (Fig. 8B), it didn't reach the statistical significance. This data is consistent with an increased inhibition in the cortex due to a higher density of PV interneurons (Fig. 1A), suggesting that PV circuits in the prefrontal cortex may contribute to CTNNB1 cKO mediated behavioral changes.

Discussion

Our results demonstrate that deleting CTNNB1 in PV interneurons significantly disrupts social and cognitive functions. This study provides the important evidence of CTNNB1's role in the inhibitory circuit *in vivo*. Our data links a deficit of CTNNB1 in PV interneurons directly to autistic-like behaviors. First, cKO of CTNNB1 in the PV interneurons causes anxiogenic effect in the OFT and EPM, but does not elicit depression-like behaviors, which is consistent with the increased anxiety in patients with ASD (55). Second, CTNNB1 cKO alters multiple cognitive functions. In particular, CTNNB1 loss-of-function impairs long-term memory in the NOR test and fear extinction. However, short-term memory in the NOR and fear memory remain intact. Intriguingly, spatial memory is enhanced by CTNNB1 cKO in PV interneurons. Third, KO of CTNNB1 in the PV interneurons leads to deficit in social interaction and increased repetitive behaviors that mimic core symptoms of ASD patients. Moreover, neuronal

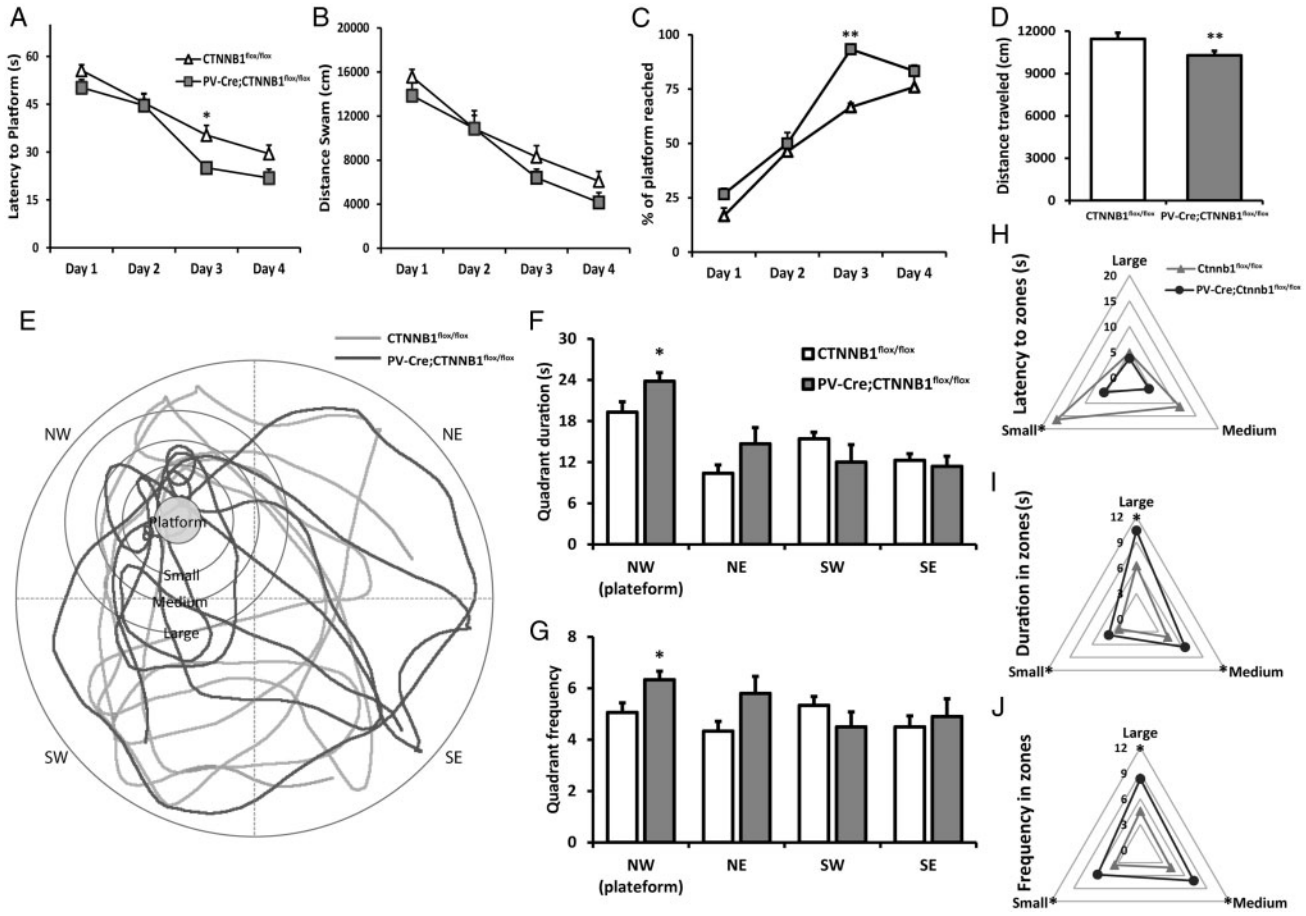

Figure 5. Spatial memory was enhanced in PV-Cre; CTNNB1$^{flox/flox}$ mice. **(A)** The accuracy of both groups to reach the platform increased with training. However, PV-Cre; CTNNB1$^{flox/flox}$ mice took less time to reach the platform. **(B)** PV-Cre; CTNNB1$^{flox/flox}$ mice took short distances to reach the platform. **(C)** The percentage of reaching the platform within 60 s was higher in CTNNB1 cKO group. **(D)** On the testing day, total distance traveled significantly decreased in PV-Cre; CTNNB1$^{flox/flox}$ mice. **(E)** Schematics show the representative traces of mouse movement in the MWM. **(F)** CTNNB1 cKO mice spent longer duration in the platform quadrant. **(G)** CTNNB1 cKO mice entered more frequently into the platform quadrant. **(H)** To better evaluate the performance of mice, we generated three concentric circles around the platform with different diameters as shown in (E). PV-Cre; CTNNB1$^{flox/flox}$ mice took shorter latency to the smallest zone. **(I)** PV-Cre; CTNNB1$^{flox/flox}$ mice spent longer duration in the smallest zone. **(J)** PV-Cre; CTNNB1$^{flox/flox}$ mice entered more into the smallest zone. *$P < 0.05$, **$P < 0.01$.

activation was significantly reduced in the cortex of cKO mice. Thus, these results support that an optimal level of CTNNB1 in either inhibitory or excitatory neurons is critical to keep normal cognitive and emotional functions.

Different from the phenotypes observed in mice with CTNNB1 KO in excitatory neurons (25), which exhibit depression-like behavior, but not anxiety-related behaviors, we found that PV interneuron-specific cKO leads to increased anxiety without depression phenotype. PV+interneurons are fast-spiking neurons that inhibit excitatory activity. Our data suggest that CTNNB1 in the inhibitory circuit controls opposite behaviors observed in the excitatory circuit. Consistently, CTNNB1 in the nucleus accumbens confers pro-resilient and anxiolytic effects through a microRNA-dependent mechanism (56), supporting a critical role of CTNNB1 in regulating anxiety. Furthermore, CTNNB1 stability is controlled by GSK3β, which is implicated in mental illness. Lithium, a widely-used mood stabilizer for patients with bipolar disorder, inhibits GSK3β *in vivo* (57). GSK3β is a major mediator of anxiety and the lithium effect (58,59). Overexpression of CTNNB1 in the mouse brain phenocopies the anti-depressant effects of lithium in the amphetamine model (60), suggesting that lithium modulates behaviors through the GSK3β-CTNNB1 pathway. Our data, together with these studies, demonstrate that an optimal level of CTNNB1 in both excitatory neurons and inhibitory neurons is critical for normal emotional behaviors.

Here we showed that a novel role of CTNNB1 in PV interneurons to modulate social interaction and spatial learning. PV interneurons control the synchronization of the brain activities and are essential in learning behaviors. Imbalance of excitation and inhibition has been implicated in multiple psychiatric disorders, such as schizophrenia (61,62) and ASDs. Consistent with its critical role in memory, we found that PV interneuron-specific KO causes deficits in objective recognition and social memory. The short-term memory and contextual fear learning in PV interneuron-specific cKO mice were not affected, suggesting that memory acquisition was intact. Interestingly, the results that CTNNB1 PV-KO mice failed to recognize the second novel object in the NOR test and the second stranger mouse in the SIT, as well as to extinguish fear memory, indicate a deficit in the ability to acquire new information and to replace previous memories. This cognitive inflexibility is seen in autistic patients (63,64) and is consistent with phenotypes of mice expressing stabilized CTNNB1 during reversal learning tasks (24). Intriguingly, our mouse model showed enhanced spatial memory, which is consistent with other autistic mouse models

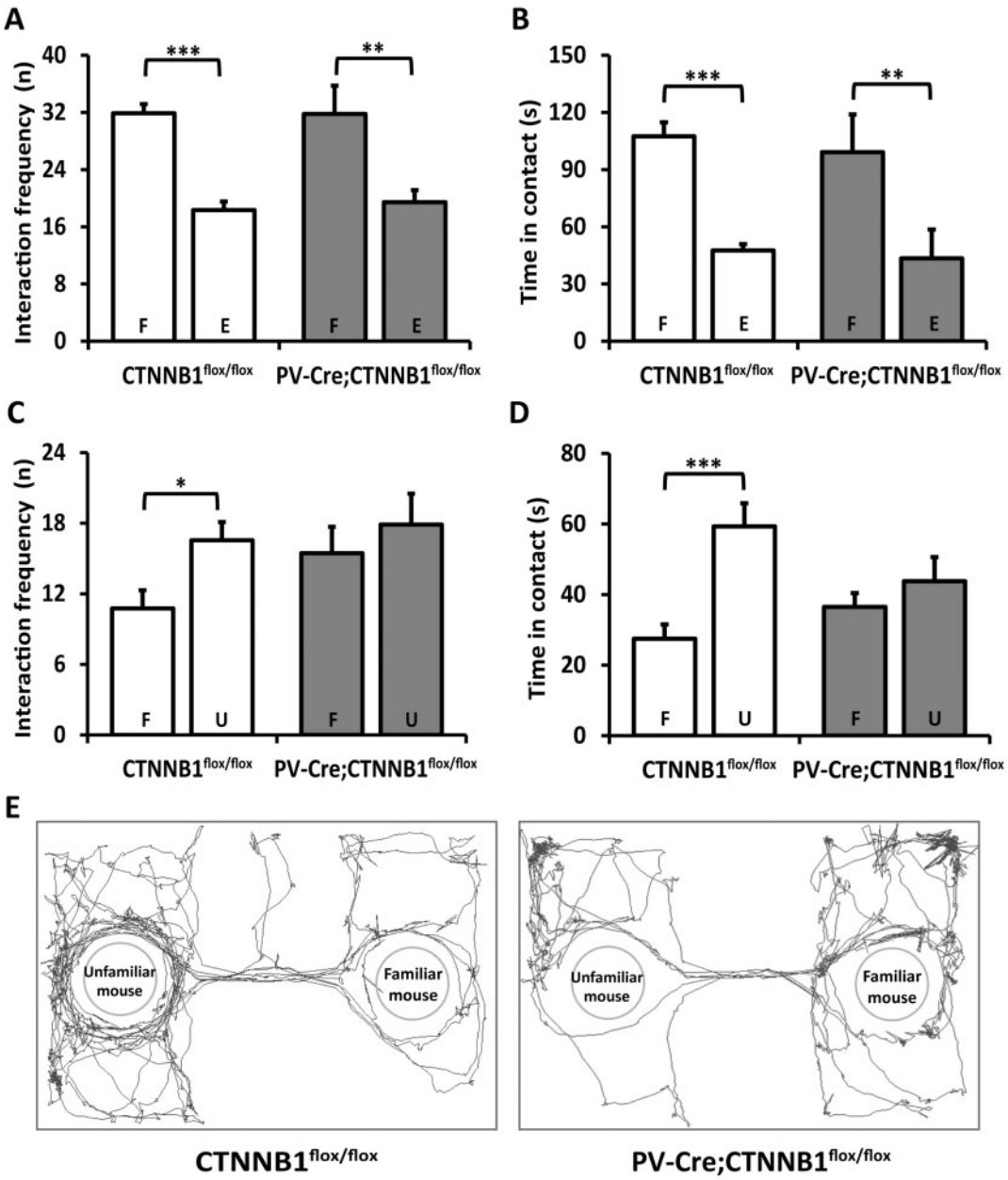

Figure 6. Social memory deficits in PV-Cre; CTNNB1$^{flox/flox}$ mice. **(A)** In the first section of SIT, both groups interacted with a mouse more frequently than the empty chamber. **(B)** Both groups spent longer time with a mouse frequently than the empty chamber. **(C)** In the second section of SIT, an unfamiliar mouse was introduced in the empty chamber. CTNNB1$^{flox/flox}$ mice was prone to interact with unfamiliar mice more frequently, but PV-Cre; CTNNB1$^{flox/flox}$ mice failed to differentiate the familiar mouse and the unfamiliar mouse. **(D)** PV-Cre; CTNNB1$^{flox/flox}$ mice spent similar time with familiar mice and unfamiliar mice. **(E)** Schematics showed the representative traces of mouse movement. Data shown are mean ± SEM from the CTNNB1$^{flox/flox}$ (N = 18) and PV-Cre; CTNNB1$^{flox/flox}$ groups (N = 10). $^{*}P < 0.05$, $^{**}P < 0.01$, $^{***}P < 0.001$. E, empty chamber;F, familiar mouse; U, unfamiliar mouse.

with defect in Shank1 (49) and neuroligin-3 (45), but not with others (46,65). Increased spatial memory could be a CTNNB1 specific effect. However, patients with ASDs can display normal or, rarely, even enhanced cognitive abilities (66,67). Thus, we cannot exclude the possibility that this alteration by CTNNB1 KO could contribute to ASD pathophysiology as the genetics and symptoms of ASDs are quite heterogeneous.

Our study indicates that CTNNB1 cKO in PV interneurons is sufficient to modify the circuit development, resulting in more PV interneurons localizing in the cortex region even though PV is mainly expressed postnatally. CTNNB1 is the key mediator in the canonical Wnt signaling pathway, which involves a variety of cellular processes, including development, cell proliferation, cell survival, and motility. During early neurodevelopment, CTNNB1 fine-tunes the balance of proliferation and differentiation of neural stem cells. Both loss- and gain-of-function of CTNNB1 resulted in neurodevelopmental deficits (8,10). Additionally, the Wnt signaling pathway controls interneuron differentiation (68), thereby balancing the excitatory and inhibitory signals at a cellular level. Since PV is expressed postnatally (69), CTNNB1 does not likely work by regulating interneuron progenitor differentiation. Our data indicated that the localization of PV+ interneurons was not changed by CTNNB1 KO at P22 in the cortex. As at this age, proliferation and fate specification

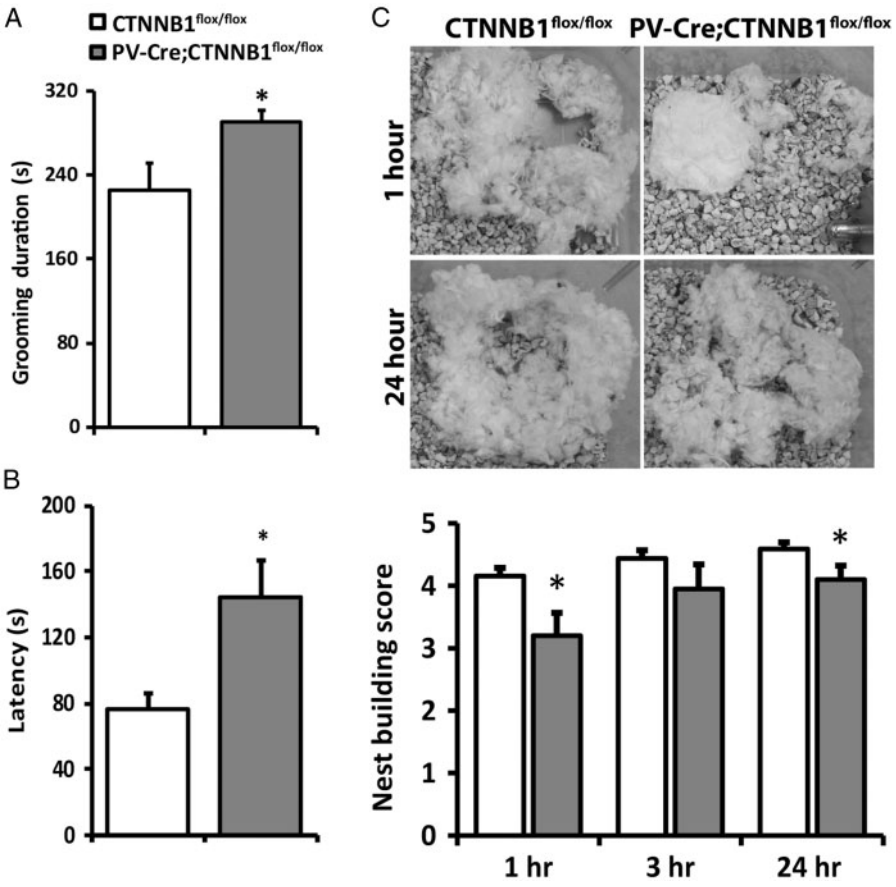

Figure 7. Abnormal repetitive behaviors in PV-Cre; CTNNB1$^{flox/flox}$ mice. **(A)** PV-Cre; CTNNB1$^{flox/flox}$ mice spent more time on grooming, which is considered a repetitive compulsive behavior. **(B)** In the MBT, PV-Cre; CTNNB1$^{flox/flox}$ mice were significantly delayed to start burying. **(C)** They performed worse in nest building than the control littermates measured at multiple times. Especially at 1 and 24 h, their scores were significantly lower than those of the controls. Data shown are mean ± SEM from Ctnnb1$^{flox/flox}$ (N = 18) and PV-Cre; Ctnnb1$^{flox/flox}$ groups (N = 10). *$P < 0.05$.

of interneuron progenitors have completed, our data suggest that mislocalization of PV cells occurs between P22 and P60, and is likely caused by a migration defect. Moreover, the number of PV+ cells in other brain regions was not changed. PV has not been shown as a direct downstream target of the Wnt pathway. This further supported that the change of PV distribution is not caused by abnormal proliferation, or altered fate determination, or modulation of PV expression. CTNNB1 might modulate migration via α-catenin-extracellular matrix interaction. However, the exact molecular mechanism on how CTNNB1 in PV neurons controls their distribution remains to be determined.

Our findings provide new insights into human CTNNB1 gene mutations in the inhibitory circuits as a risk factor for ASD/ID. Mutations in the Wnt pathway are enriched in the genetic risks in ASD (6). Consistently, mutations of CTNNB1 were identified in patients with ASD (6) and ID (9). Previous studies did not identify autistic-like behaviors, including anxiety, social interaction deficit and repetitive behaviors, on mouse models with CTNNB1 KO in excitatory neurons (22,24,25,60). Our study reveals that CTNNB1 KO in PV interneurons leads to cognitive and autistic-like phenotypes, suggesting that CTNNB1 defects in PV interneurons are responsible for the core symptoms of autistic-like behaviors. CTNNB1 interacts with α-catenin and N-cadherin to form cell adhesion complex localized at cell membrane and in synaptic junctions (21,70). It controls the synaptic strength and modulates neuronal plasticity in excitatory neurons (15,16,18,20). CTNNB1 may also regulate the electrophysiology of interneurons. Consistent with this notion, c-Fos staining was significantly reduced in the cortex, but not in the dentate gyrus and the amygdala, suggesting that an increased inhibition in the cortex, which may contribute to CTNNB1 KO-mediated behavioral changes. This data is consistent with increased inhibition in the cortex due to a higher density of PV interneurons. Future studies will be required to further delineate the underlying pathophysiological mechanisms. It would be interesting to further narrow down if CTNNB1 deletion from different brain regions or interneuron subtype will mediate particular phenotypes. Such studies will provide a better understanding of circuitry mechanism for ASD and might be potentially useful to design a new strategy to alleviate ASD symptoms.

Materials and Methods

Animals

The CTNNB1$^{flox/flox}$ mice (B6.129-CTNNB1^{tm2Kem}/*KnwJ*) and the PV-Cre mice (B6; 129P2-Pvalb$^{tm1(cre)Arbr}$/J) from the Jackson Laboratory (Bar Harbor, ME) were used to produce the heterozygous offspring. PV-Cre; CTNNB1 $^{flox/flox}$ mouse model were generated by backcrossing of F1 hybrids. All mice (two to four mice per cage) were housed at an ambient room temperature (20–22°C) with a 12-h light/12-h dark cycle (lights on at 6:00 am), and given ad libitum access to food and water. All animal

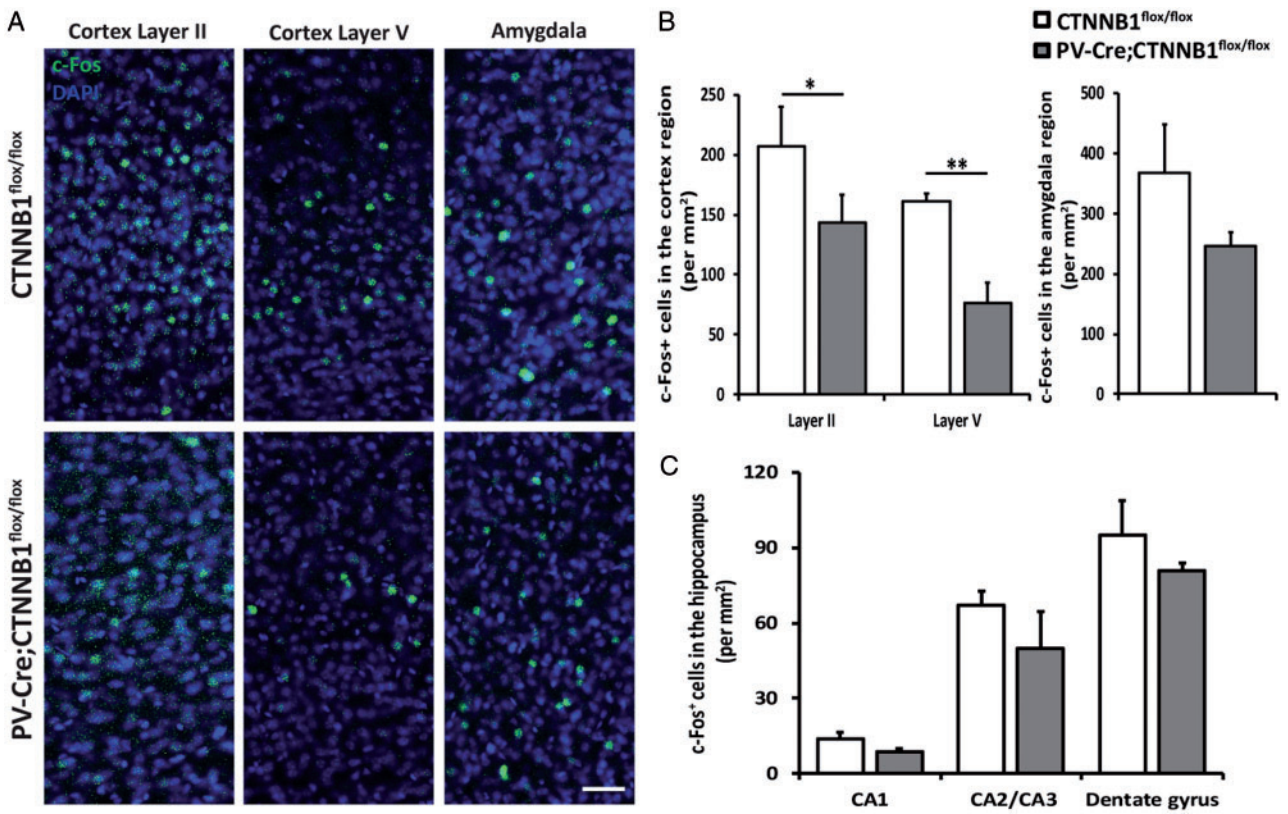

Figure 8. Abnormal neuronal activity in PV-Cre; CTNNB1$^{flox/flox}$ mice. **(A)** The number of c-Fos+ cells was significantly decreased at layer II and V of the cortex in PV-Cre; CTNNB1$^{flox/flox}$ mice. **(B)** Distribution of c-Fos+ cells at the amygdala region was not significantly changed in control and PV-Cre; CTNNB1$^{flox/flox}$ mice. **(C)** Distribution of c-Fos+ cells did not showed a significant change at the hippocampus regions. $^{*}P < 0.05$. $^{**}P < 0.01$.

experiments and procedures were reviewed and approved by The Pennsylvania State University IACUC committee.

Immunohistochemistry

Mice were anesthetized with Avertin (200 mg per kg of body weight) and perfused with artificial cerebrospinal fluid and 4% performic acid (PFA). To investigate the neuronal activity using c-Fos immunohistochemistry, mice were stimulated by three times of 2-s, 0.55-mA foot shock within 250 s and put back to the original cage. One hour after the stimulation, mice were perfused. After post-fixation with 4% PFA for 24 h, brains were sliced by vibratome at the thickness of 50 μm. Each slide was pre-blocked with 5% donkey serum and 0.2% Triton X-100 in phosphate-buffered saline (PBS) for 1 h at room temperature. Primary antibodies were mixed in fresh blocking solution and incubate with brain slides for overnight at 4°C. After washing with PBS and 0.1% Triton X-100, brain slides were incubated with secondary antibodies conjugated with fluorescent groups. Brain slides were mounted to glass slides and photographed by confocal microscope. Image J was used for analysis of images. Antibodies used in this study are: rabbit anti-c-Fos antibody (Sigma), rabbit anti-PV antibody (Synaptic Systems), mouse anti-CTNNB1 antibody (BD Transduction Laboratories).

Behavior Tests

CTNNB1$^{flox/flox}$ mice (N = 18, male = 12, female = 6) and PV-Cre; CTNNB1 $^{flox/flox}$ mice (N = 10, male = 7, female = 3) were used to test animal behaviors at adulthood (P60) (71). The mice were kept in their cages and acclimated to the behavior testing room 1 h before each test. We recorded each trial with an EthoVision XT video tracking system and software (Noldus).

Open field test

The test was conducted as described in (46) with modifications. Briefly, each individual mouse was randomly placed at one corner of an opaque, open acrylic box (40×40×40 cm) in a brightly lit room. Video camera recorded horizontal movement of the mouse for 5 min. Total distance traveled, duration and entry frequency in the center (13.3 × 13.3 cm), as well as the latency to the center region, were measured by EthoVision XT software. The open field apparatus was cleaned with 70% ethanol between each trial.

Elevated Plus Maze test

The test was performed as reported in (39). The maze is a four-armed acrylic platform with a plus shape. The platform is elevated 50 cm above the ground, and two of the arms (5 × 25 cm) were enclosed with high walls, and the other two arms were open. Each mouse was placed into the crossing region (5 × 5 cm) of open and closed arms. The arms entry frequency, latency, duration and distance traveled were measured time spent in the closed and open arms were measured by EthoVision XT video tracking system. The plus maze apparatus was cleaned with 70% ethanol between each trial.

Novel Object Recognition test

In this test, mice were at first allowed free exploration for 5 min to acclimate with the testing environment in the open field arena. After the habituation session, mice interacted with two identical objects for 5 min. At 1 h after the habituation, the novel object 1 replaced one of the familiar objects. After 24 h, another novel object replaced the novel object 1. The amount of time mice spent with each object was measured by EthoVision XT to test the short- and long-term memory. Three groups of objects were with different shape, material and color, and randomly selected to serve as familiar objects or novel objects. The testing box was cleaned with 70% ethanol between each trial.

Social interaction test

The SIT was performed as reported with modifications (72). All the mice were single housed for 1 week before the tests. Mice were allowed to habituate with the three-chamber (each 20 × 40 × 20 (h) cm) box with two empty steel wire pencil cups (diameter 7 cm, height 10 cm) placed in center of the left or right chamber for 10 min. After habituation, one gender-matched wild-type mouse was placed in one cup. The wild-type mouse has never been exposed to the test mouse. The tested mouse was allowed to interact with either the empty cup or the cup with mouse for 10 min. At the other 10-min session, a stranger mouse was placed in the empty cup to test social memory. The frequency and time spent interacting with mouse or the empty cup were measured manually. Attempting to climb over or behind the cups was not recorded as an interaction. The testing box was cleaned with 70% ethanol between each trial.

Morris water maze

The MWM was done as reported in (73) with a period of 5 days, which included four training sessions and one test session. A transparent platform with a diameter of 10 cm was placed in the center of one quadrant of the pool (diameter 150 cm). The top of the platform was placed 2 cm below the water surface. Three other quadrants were labeled with different sign using color tapes for providing mice position cues. Nontoxic white watercolor paint was mixed into the water until the platform was no longer visible.

On training days, each mouse was placed into a randomly selected quadrant of the pool (a random number generator provided a number from one to four). If the mouse did not find the platform within 60 s, it was guided there by hand and allowed to stay there for 15 s. This was repeated three times daily for all the mice. On the testing day, the platform was removed and a circular platform zone was marked in the EthoVision software. The mice were individually placed into the pool and allowed to search for the platform. The times spent in the platform zone, as well as three larger circles concentric to the zone, were measured manually from the recorded videos. Quadrant duration and enter frequency were measured by EthoVision TX. All data are shown as mean ± SEM and analyzed by Student's two-tailed, unpaired *t*-test.

Grooming test

This test was used to score the repetitive behaviors (74). Each mouse was misted with a spray of distilled water towards to its face and placed into an empty cage without bedding. The animals were filmed for 25 min each. Accumulated grooming time was measured manually from the video. The first 5 min were excluded from the analysis because the variations in grooming duration during that time seemed largely dependent on the amount of water with which the mouse had been misted.

Marble burying test

This test was performed as reported in (75). Each mouse was placed into a new cage with 3 cm of bedding and five rows of four marbles on the surface of bedding. Leaving the mice in the testing cages for 10 min, we counted the number of marble buried and measured the latency to the first bury. All data are shown as mean ± SEM and analyzed by Mann-Whitney U test.

Tail suspension test

Each mouse was secured to a horizontal rod about 60 cm above the floor using the end of its tail. The mouse was recorded for 5 min. Immobility time (when the mouse did not curl, move its paws, or swing across its vertical axis) (76) was measured manually from the video with a stopwatch.

Rotarod test

This test was done to exclude the possibility of motor deficits in Cre-positive mice that may result in misleading behavior test results (77). Each mouse was placed on the apparatus at four revolutions per minute (RPM). The speed accelerates from 4 RPM to a max of 40 RPM in 5 min, and the maximum speed is maintained for 5 min. We recorded the falling time of each mouse, and repeat the procedure three times per day for 3 days. On the eighth day, mice were tested with the same procedure. The rotarod apparatus was cleaned with 70% ethanol between each trial.

Nest building test

This test was performed as described in (78). Single-housed mice were transferred to new cages with 2 g nestlet in each cage. Assess the nests after 1, 3, and 24 h on a rating scale of 1–5. Scores were analyzed using Kruskal-Wallis ANOVA.

Fear conditioning and extinction test

In the training session, each mouse was habituated in the fear conditioning apparatus for 5 min. After the habituation, the mouse in the testing chamber will receive a 2-s, 0.55-mA foot shock every 80 s (79). The mouse was removed immediately after the third shock. During the contextual testing, the freezing behavior of each mouse was recorded in the testing chamber every 24 h until reaching the significant difference between two groups.

Statistical Analysis

Data were analyzed using Excel and SPSS software and are expressed as means ± SEM. Significances between the experimental group and control group were analyzed by Student's *t*-test and ANOVA.

Supplementary Material

Supplementary Material is available at *HMG* online.

Acknowledgements

We thank Ms Siying Zhu and Dr Bernhard Luscher, Dr Timothy Jegla and Dr Gong Chen for the technical support. Dr Yingwei Mao is a receipt of NARSAD Young Investigator Award and American Heart Scientist Development Award. We thank Gary Howard for suggestions.

Conflict of Interest statement. None declared.

Funding

Funding to pay the Open Access publication charges for this article was provided by Research Foundation of National University of Defense Technology to Dr. Long Liu, JC-14-02-01.

References

1. Williams, D.L., Goldstein, G. and Minshew, N.J. (2006) Neuropsychologic functioning in children with autism: further evidence for disordered complex information-processing. *Child Neuropsychol.*, **12**, 279–298.
2. van Steensel, F.J., Bogels, S.M. and Perrin, S. (2011) Anxiety disorders in children and adolescents with autistic spectrum disorders: a meta-analysis. *Clin. Child Fam. Psychol. Rev.*, **14**, 302–317.
3. Williams, D.L., Goldstein, G. and Minshew, N.J. (2006) The profile of memory function in children with autism. *Neuropsychology*, **20**, 21–29.
4. Miles, J.H. (2011) Autism spectrum disorders–a genetics review. *Genet. Med.*, **13**, 278–294.
5. Sanders, S.J., He, X., Willsey, A.J., Ercan-Sencicek, A.G., Samocha, K.E., Cicek, A.E., Murtha, M.T., Bal, V.H., Bishop, S.L., Dong, S. *et al.* (2015) Insights into autism spectrum disorder genomic architecture and biology from 71 risk loci. *Neuron*, **87**, 1215–1233.
6. O'Roak, B.J., Vives, L., Girirajan, S., Karakoc, E., Krumm, N., Coe, B.P., Levy, R., Ko, A., Lee, C., Smith, J.D. *et al.* (2012) Sporadic autism exomes reveal a highly interconnected protein network of de novo mutations. *Nature*, **485**, 246–250.
7. Brembeck, F.H., Rosario, M. and Birchmeier, W. (2006) Balancing cell adhesion and Wnt signaling, the key role of beta-catenin. *Curr. Opin. Genet. Dev.*, **16**, 51–59.
8. Haegel, H., Larue, L., Ohsugi, M., Fedorov, L., Herrenknecht, K. and Kemler, R. (1995) Lack of beta-catenin affects mouse development at gastrulation. *Development*, **121**, 3529–3537.
9. de Ligt, J., Willemsen, M.H., van Bon, B.W., Kleefstra, T., Yntema, H.G., Kroes, T., Vulto-van Silfhout, A.T., Koolen, D.A., de Vries, P., Gilissen, C. *et al.* (2012) Diagnostic exome sequencing in persons with severe intellectual disability. *N. Engl. J. Med.*, **367**, 1921–1929.
10. Chenn, A. and Walsh, C.A. (2002) Regulation of cerebral cortical size by control of cell cycle exit in neural precursors. *Science*, **297**, 365–369.
11. Zechner, D., Fujita, Y., Hulsken, J., Muller, T., Walther, I., Taketo, M.M., Crenshaw, E.B., 3rd, Birchmeier, W. and Birchmeier, C. (2003) beta-Catenin signals regulate cell growth and the balance between progenitor cell expansion and differentiation in the nervous system. *Dev. Biol.*, **258**, 406–418.
12. Brault, V., Moore, R., Kutsch, S., Ishibashi, M., Rowitch, D.H., McMahon, A.P., Sommer, L., Boussadia, O. and Kemler, R. (2001) Inactivation of the beta-catenin gene by Wnt1-Cre-mediated deletion results in dramatic brain malformation and failure of craniofacial development. *Development*, **128**, 1253–1264.
13. Yu, X. and Malenka, R.C. (2003) Beta-catenin is critical for dendritic morphogenesis. *Nat. Neurosci.*, **6**, 1169–1177.
14. Tan, Z.J., Peng, Y., Song, H.L., Zheng, J.J. and Yu, X. (2010) N-cadherin-dependent neuron-neuron interaction is required for the maintenance of activity-induced dendrite growth. *Proc. Natl. Acad. Sci. U S A*, **107**, 9873–9878.
15. Murase, S., Mosser, E. and Schuman, E.M. (2002) Depolarization drives beta-Catenin into neuronal spines promoting changes in synaptic structure and function. *Neuron*, **35**, 91–105.
16. Bian, W.J., Miao, W.Y., He, S.J., Qiu, Z. and Yu, X. (2015) Coordinated Spine Pruning and Maturation Mediated by Inter-Spine Competition for Cadherin/Catenin Complexes. *Cell*, **162**, 808–822.
17. Peng, Y.R., He, S., Marie, H., Zeng, S.Y., Ma, J., Tan, Z.J., Lee, S.Y., Malenka, R.C. and Yu, X. (2009) Coordinated changes in dendritic arborization and synaptic strength during neural circuit development. *Neuron*, **61**, 71–84.
18. Okuda, T., Yu, L.M., Cingolani, L.A., Kemler, R. and Goda, Y. (2007) beta-Catenin regulates excitatory postsynaptic strength at hippocampal synapses. *Proc. Natl. Acad. Sci. U S A*, **104**, 13479–13484.
19. Taylor, A.M., Wu, J., Tai, H.C. and Schuman, E.M. (2013) Axonal translation of beta-catenin regulates synaptic vesicle dynamics. *J. Neurosci.*, **33**, 5584–5589.
20. Bamji, S.X., Shimazu, K., Kimes, N., Huelsken, J., Birchmeier, W., Lu, B. and Reichardt, L.F. (2003) Role of beta-catenin in synaptic vesicle localization and presynaptic assembly. *Neuron*, **40**, 719–731.
21. Bamji, S.X., Rico, B., Kimes, N. and Reichardt, L.F. (2006) BDNF mobilizes synaptic vesicles and enhances synapse formation by disrupting cadherin-beta-catenin interactions. *J. Cell. Biol.*, **174**, 289–299.
22. Maguschak, K.A. and Ressler, K.J. (2008) Beta-catenin is required for memory consolidation. *Nat. Neurosci.*, **11**, 1319–1326.
23. Tucci, V., Kleefstra, T., Hardy, A., Heise, I., Maggi, S., Willemsen, M.H., Hilton, H., Esapa, C., Simon, M., Buenavista, M.T., *et al.* (2014) Dominant beta-catenin mutations cause intellectual disability with recognizable syndromic features. *J. Clin. Invest.*, **124**, 1468–1482.
24. Mills, F., Bartlett, T.E., Dissing-Olesen, L., Wisniewska, M.B., Kuznicki, J., Macvicar, B.A., Wang, Y.T. and Bamji, S.X. (2014) Cognitive flexibility and long-term depression (LTD) are impaired following beta-catenin stabilization in vivo. *Proc. Natl. Acad. Sci. U S A*, **111**, 8631–8636.
25. Gould, T.D., O'Donnell, K.C., Picchini, A.M., Dow, E.R., Chen, G. and Manji, H.K. (2008) Generation and behavioral characterization of beta-catenin forebrain-specific conditional knock-out mice. *Behav. Brain Res.*, **189**, 117–125.
26. Mohn, J.L., Alexander, J., Pirone, A., Palka, C.D., Lee, S.Y., Mebane, L., Haydon, P.G. and Jacob, M.H. (2014) Adenomatous polyposis coli protein deletion leads to cognitive and autism-like disabilities. *Mol. Psychiatry*, **19**, 1133–1142.
27. Kwon, C.H., Luikart, B.W., Powell, C.M., Zhou, J., Matheny, S.A., Zhang, W., Li, Y., Baker, S.J. and Parada, L.F. (2006) Pten regulates neuronal arborization and social interaction in mice. *Neuron*, **50**, 377–388.
28. Sato, A., Kasai, S., Kobayashi, T., Takamatsu, Y., Hino, O., Ikeda, K. and Mizuguchi, M. (2012) Rapamycin reverses impaired social interaction in mouse models of tuberous sclerosis complex. *Nat. Commun.*, **3**, 1292.
29. Hu, H., Gan, J. and Jonas, P. (2014) Interneurons. Fast-spiking, parvalbumin(+) GABAergic interneurons: from cellular design to microcircuit function. *Science*, **345**, 1255263.

30. Lawrence, Y.A., Kemper, T.L., Bauman, M.L. and Blatt, G.J. (2010) Parvalbumin-, calbindin-, and calretinin-immunoreactive hippocampal interneuron density in autism. *Acta Neurol. Scand.*, **121**, 99–108.
31. Blatt, G.J. and Fatemi, S.H. (2011) Alterations in GABAergic biomarkers in the autism brain: research findings and clinical implications. *Anat. Rec. (Hoboken)*, **294**, 1646–1652.
32. Yip, J., Soghomonian, J.J. and Blatt, G.J. (2008) Increased GAD67 mRNA expression in cerebellar interneurons in autism: implications for Purkinje cell dysfunction. *J. Neurosci. Res.*, **86**, 525–530.
33. Yip, J., Soghomonian, J.J. and Blatt, G.J. (2009) Decreased GAD65 mRNA levels in select subpopulations of neurons in the cerebellar dentate nuclei in autism: an in situ hybridization study. *Autism Res.*, **2**, 50–59.
34. Gogolla, N., Leblanc, J.J., Quast, K.B., Sudhof, T.C., Fagiolini, M. and Hensch, T.K. (2009) Common circuit defect of excitatory-inhibitory balance in mouse models of autism. *J. Neurodev. Disord.*, **1**, 172–181.
35. Councill, J.H., Tucker, E.S., Haskell, G.T., Maynard, T.M., Meechan, D.W., Hamer, R.M., Lieberman, J.A. and LaMantia, A.S. (2006) Limited influence of olanzapine on adult forebrain neural precursors in vitro. *Neuroscience*, **140**, 111–122.
36. Wohr, M., Orduz, D., Gregory, P., Moreno, H., Khan, U., Vorckel, K.J., Wolfer, D.P., Welzl, H., Gall, D., Schiffmann, S.N. *et al.* (2015) Lack of parvalbumin in mice leads to behavioral deficits relevant to all human autism core symptoms and related neural morphofunctional abnormalities. *Transl. Psychiatry*, **5**, e525.
37. Marin, O. (2012) Interneuron dysfunction in psychiatric disorders. *Nat. Rev. Neurosci.*, **13**, 107–120.
38. Davila, J.C., Real, M.A., Olmos, L., Legaz, I., Medina, L. and Guirado, S. (2005) Embryonic and postnatal development of GABA, calbindin, calretinin, and parvalbumin in the mouse claustral complex. *J. Comp. Neurol.*, **481**, 42–57.
39. Walf, A.A. and Frye, C.A. (2007) The use of the elevated plus maze as an assay of anxiety-related behavior in rodents. *Nat. Protoc.*, **2**, 322–328.
40. Takeda, H., Tsuji, M. and Matsumiya, T. (1998) Changes in head-dipping behavior in the hole-board test reflect the anxiogenic and/or anxiolytic state in mice. *Eur. J. Pharmacol.*, **350**, 21–29.
41. Steru, L., Chermat, R., Thierry, B. and Simon, P. (1985) The tail suspension test: a new method for screening antidepressants in mice. *Psychopharmacology (Berl)*, **85**, 367–370.
42. Donato, F., Rompani, S.B. and Caroni, P. (2013) Parvalbumin-expressing basket-cell network plasticity induced by experience regulates adult learning. *Nature*, **504**, 272–276.
43. Courtin, J., Chaudun, F., Rozeske, R.R., Karalis, N., Gonzalez-Campo, C., Wurtz, H., Abdi, A., Baufreton, J., Bienvenu, T.C. and Herry, C. (2014) Prefrontal parvalbumin interneurons shape neuronal activity to drive fear expression. *Nature*, **505**, 92–96.
44. Pitts, M.W., Raman, A.V., Hashimoto, A.C., Todorovic, C., Nichols, R.A. and Berry, M.J. (2012) Deletion of selenoprotein P results in impaired function of parvalbumin interneurons and alterations in fear learning and sensorimotor gating. *Neuroscience*, **208**, 58–68.
45. Tabuchi, K., Blundell, J., Etherton, M.R., Hammer, R.E., Liu, X., Powell, C.M. and Sudhof, T.C. (2007) A neuroligin-3 mutation implicated in autism increases inhibitory synaptic transmission in mice. *Science*, **318**, 71–76.
46. Han, S., Tai, C., Westenbroek, R.E., Yu, F.H., Cheah, C.S., Potter, G.B., Rubenstein, J.L., Scheuer, T., de la Iglesia, H.O. and Catterall, W.A. (2012) Autistic-like behaviour in Scn1a+/- mice and rescue by enhanced GABA-mediated neurotransmission. *Nature*, **489**, 385–390.
47. Blundell, J., Blaiss, C.A., Etherton, M.R., Espinosa, F., Tabuchi, K., Walz, C., Bolliger, M.F., Sudhof, T.C. and Powell, C.M. (2010) Neuroligin-1 deletion results in impaired spatial memory and increased repetitive behavior. *J. Neurosci.*, **30**, 2115–2129.
48. Moretti, P., Levenson, J.M., Battaglia, F., Atkinson, R., Teague, R., Antalffy, B., Armstrong, D., Arancio, O., Sweatt, J.D. and Zoghbi, H.Y. (2006) Learning and memory and synaptic plasticity are impaired in a mouse model of Rett syndrome. *J. Neurosci.*, **26**, 319–327.
49. Hung, A.Y., Futai, K., Sala, C., Valtschanoff, J.G., Ryu, J., Woodworth, M.A., Kidd, F.L., Sung, C.C., Miyakawa, T., Bear, M.F., *et al.* (2008) Smaller dendritic spines, weaker synaptic transmission, but enhanced spatial learning in mice lacking Shank1. *J. Neurosci.*, **28**, 1697–1708.
50. Hedlund, P.B. and Sutcliffe, J.G. (2007) The 5-HT7 receptor influences stereotypic behavior in a model of obsessive-compulsive disorder. *Neurosci. Lett.*, **414**, 247–251.
51. Moy, S.S., Nadler, J.J., Young, N.B., Perez, A., Holloway, L.P., Barbaro, R.P., Barbaro, J.R., Wilson, L.M., Threadgill, D.W., Lauder, J.M. *et al.* (2007) Mouse behavioral tasks relevant to autism: phenotypes of 10 inbred strains. *Behav. Brain Res.*, **176**, 4–20.
52. Deacon, R.M., Croucher, A. and Rawlins, J.N. (2002) Hippocampal cytotoxic lesion effects on species-typical behaviours in mice. *Behav. Brain Res.*, **132**, 203–213.
53. Slotnick, B.M. and Nigrosh, B.J. (1975) Maternal behavior of mice with cingulate cortical, amygdala, or septal lesions. *J. Comp. Physiol. Psychol.*, **88**, 118–127.
54. Allsop, S.A., Vander Weele, C.M., Wichmann, R. and Tye, K.M. (2014) Optogenetic insights on the relationship between anxiety-related behaviors and social deficits. *Front. Behav. Neurosci.*, **8**, 241.
55. Wilcox, J.A., Tsuang, M.T., Schnurr, T. and Baida-Fragoso, N. (2003) Case-control family study of lesser variant traits in autism. *Neuropsychobiology*, **47**, 171–177.
56. Dias, C., Feng, J., Sun, H., Shao, N.Y., Mazei-Robison, M.S., Damez-Werno, D., Scobie, K., Bagot, R., LaBonte, B., Ribeiro, E., *et al.* (2015) beta-catenin mediates stress resilience through Dicer1/microRNA regulation. *Nature*, **516**, 51–55.
57. Gould, T.D., Chen, G. and Manji, H.K. (2004) In vivo evidence in the brain for lithium inhibition of glycogen synthase kinase-3. *Neuropsychopharmacology*, **29**, 32–38.
58. Latapy, C., Rioux, V., Guitton, M.J. and Beaulieu, J.M. (2012) Selective deletion of forebrain glycogen synthase kinase 3beta reveals a central role in serotonin-sensitive anxiety and social behaviour. *Philos. Trans. R Soc. Lond. B Biol. Sci.*, **367**, 2460–2474.
59. O'Brien, W.T., Harper, A.D., Jove, F., Woodgett, J.R., Maretto, S., Piccolo, S. and Klein, P.S. (2004) Glycogen synthase kinase-3beta haploinsufficiency mimics the behavioral and molecular effects of lithium. *J. Neurosci.*, **24**, 6791–6798.
60. Gould, T.D., Einat, H., O'Donnell, K.C., Picchini, A.M., Schloesser, R.J. and Manji, H.K. (2007) Beta-catenin overexpression in the mouse brain phenocopies lithium-sensitive behaviors. *Neuropsychopharmacology*, **32**, 2173–2183.
61. Beneyto, M. and Lewis, D.A. (2011) Insights into the neurodevelopmental origin of schizophrenia from postmortem studies of prefrontal cortical circuitry. *Int. J. Dev. Neurosci.*, **29**, 295–304.

62. Gonzalez-Burgos, G., Cho, R.Y. and Lewis, D.A. (2015) Alterations in cortical network oscillations and parvalbumin neurons in schizophrenia. *Biol. Psychiatry*, **77**, 1031–1040.
63. Yasuda, Y., Hashimoto, R., Ohi, K., Yamamori, H., Fujimoto, M., Umeda-Yano, S., Fujino, H. and Takeda, M. (2014) Cognitive inflexibility in Japanese adolescents and adults with autism spectrum disorders. *World J. Psychiatry*, **4**, 42–48.
64. Granader, Y., Wallace, G.L., Hardy, K.K., Yerys, B.E., Lawson, R.A., Rosenthal, M., Wills, M.C., Dixon, E., Pandey, J., Penna, R. *et al.* (2014) Characterizing the factor structure of parent reported executive function in autism spectrum disorders: the impact of cognitive inflexibility. *J. Autism Dev. Disord.*, **44**, 3056–3062.
65. Ehninger, D., Han, S., Shilyansky, C., Zhou, Y., Li, W., Kwiatkowski, D.J., Ramesh, V. and Silva, A.J. (2008) Reversal of learning deficits in a Tsc2+/- mouse model of tuberous sclerosis. *Nat. Med.*, **14**, 843.
66. Joseph, R.M., Keehn, B., Connolly, C., Wolfe, J.M. and Horowitz, T.S. (2009) Why is visual search superior in autism spectrum disorder? *Dev. Sci.*, **12**, 1083–1096.
67. Caron, M.J., Mottron, L., Rainville, C. and Chouinard, S. (2004) Do high functioning persons with autism present superior spatial abilities? *Neuropsychologia*, **42**, 467–481.
68. Paina, S., Garzotto, D., DeMarchis, S., Marino, M., Moiana, A., Conti, L., Cattaneo, E., Perera, M., Corte, G., Calautti, E., *et al.* (2011) Wnt5a is a transcriptional target of Dlx homeogenes and promotes differentiation of interneuron progenitors in vitro and in vivo. *J. Neurosci.*, **31**, 2675–2687.
69. de Lecea, L., del Rio, J.A. and Soriano, E. (1995) Developmental expression of parvalbumin mRNA in the cerebral cortex and hippocampus of the rat. *Brain Res. Mol. Brain Res.*, **32**, 1–13.
70. Tai, C.Y., Mysore, S.P., Chiu, C. and Schuman, E.M. (2007) Activity-regulated N-cadherin endocytosis. *Neuron*, **54**, 771–785.
71. Rademakers, R., Sleegers, K., Theuns, J., Van den Broeck, M., Bel Kacem, S., Nilsson, L.G., Adolfsson, R., van Duijn, C.M., Van Broeckhoven, C. and Cruts, M. (2005) Association of cyclin-dependent kinase 5 and neuronal activators p35 and p39 complex in early-onset Alzheimer's disease. *Neurobiol. Aging*, **26**, 1145–1151.
72. Terzian, A.L., Drago, F., Wotjak, C.T. and Micale, V. (2011) The dopamine and cannabinoid interaction in the modulation of emotions and cognition: assessing the role of cannabinoid CB1 receptor in neurons expressing dopamine D1 receptors. *Front. Behav. Neurosci.*, **5**, 49.
73. Vorhees, C.V. and Williams, M.T. (2006) Morris water maze: procedures for assessing spatial and related forms of learning and memory. *Nat. Protoc.*, **1**, 848–858.
74. Kalueff, A.V., Aldridge, J.W., LaPorte, J.L., Murphy, D.L. and Tuohimaa, P. (2007) Analyzing grooming microstructure in neurobehavioral experiments. *Nat. Protoc.*, **2**, 2538–2544.
75. Deacon, R.M. (2006) Digging and marble burying in mice: simple methods for in vivo identification of biological impacts. *Nat. Protoc.*, **1**, 122–124.
76. Berrocoso, E., Ikeda, K., Sora, I., Uhl, G.R., Sanchez-Blazquez, P. and Mico, J.A. (2013) Active behaviours produced by antidepressants and opioids in the mouse tail suspension test. *Int. J. Neuropsychopharmacol.*, **16**, 151–162.
77. Shiotsuki, H., Yoshimi, K., Shimo, Y., Funayama, M., Takamatsu, Y., Ikeda, K., Takahashi, R., Kitazawa, S. and Hattori, N. (2010) A rotarod test for evaluation of motor skill learning. *J. Neurosci. Methods*, **189**, 180–185.
78. Deacon, R.M. (2006) Assessing nest building in mice. *Nat. Protoc.*, **1**, 1117–1119.
79. Pollak, D.D., Monje, F.J. and Lubec, G. (2010) The learned safety paradigm as a mouse model for neuropsychiatric research. *Nat. Protoc.*, **5**, 954–962.